

Movable Thomson Scattering System Based on Optical Fiber (TS-probe)

K. Narihara, H. Hayashi

National Institute for Fusion Science, 322-6 Oroshi-cho, Toki 509-5292, Japan

(Received day month year / Accepted day month year)

This paper proposes a movable compact Thomson scattering (TS) system based on optical fibers (TS-probe). A TS-probe consists of a probe head, optical fiber, laser-diode, polychromators and lock-in amplifiers. A laser beam optics and light collection optics are mounted rigidly on a probe head with a fixed scattering position. Laser light and scattered light are transmitted by flexible optical fibers, enabling us to move the TS-probe head freely during plasma discharge. The light signal scattered from an amplitude-modulated laser is detected against the plasma light based on the principle of the lock-in amplifier. With a modulated laser power of 300W, the scattered signal from a sheet plasma of 15 mm depth and $n_e \sim 10^{19} \text{ m}^{-3}$ will be measured with 10% accuracy by setting the integrating time to 0.1 s. The TS-probe head is like a 1/20 model of the currently operating LHD-TS.

Keywords: Thomson scattering system, fiber laser, divertor plasma, TS-probe, LHD

1. Introduction

In fusion-oriented plasma experiments, Thomson scattering (TS) is a standard method to obtain electron temperature (T_e) and density (n_e) profile data. Its advantage lies in that it gives local values of T_e and n_e with a high confidence and accuracy. There are, however, disadvantages: the small probability of TS ($n_e \sigma_L < 10^{-11}$) necessitates bright optics and high efficient detectors even with the currently available high-energy pulse lasers; and precise laser beam alignment is often required. As a result of these, a TS usually requires a high cost and tedious labor in construction and maintenance, which preventing an easy use of TS at various locations in a plasma confinement device. As an example of a way out of this disadvantageous situation, this paper proposes an idea of a "TS-probe" which is compact and movable, like a Lagmuire probe, to a desired position around a plasma without necessity of laser beam alignment. We have already proposed a similar idea 13 years ago [1], but it have not yet realized ~~because of absence of the suitable optical~~

author's e-mail: narihara@nifs.ac.jp

components. With recent substantial progresses in the necessary optical components, we reexamine the idea in this paper.

2. Description of a TS-probe

A schematic view of a TS-probe designed for measuring a divertor-leg plasma of 15 mm depth is given in Fig. 1.

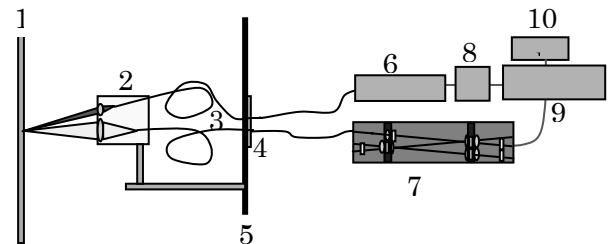


Fig.1. Schematic view of a TS-probe: 1. divertor-leg plasma; 2. TS-probe head; 3. optical fibers; 4. fiber feed-through; 5. vacuum chamber wall; 6. laser diode; 7. polychromator; 8. pulse generator; 9. lock-in amplifier; 10. data acquisition and computer.

It consists of: a probe head; optical fibers; optical fiber feed-through; laser diode; polychromator; lock-in amplifiers. These are described in details in what follows.

(1) A probe head delivers laser energy and collects a backwardly scattered light from a fixed scattering position. A key point is to collect as many TS-photons as possible while keeping background plasma light at the smallest level. For this, it is important to form the image of the laser beam just onto the surface of the light collection fiber with a well-adjusted size slit. Figure 2 shows the scattering configuration. From a simple geometry, the image of the oblique line (laser beam), which intersects the L2's optical axis at the angle α , intersects the optical axis at β , which are related by $\tan\alpha/\tan\beta=m$. Here $m=75/175=1/2$ is the magnification.

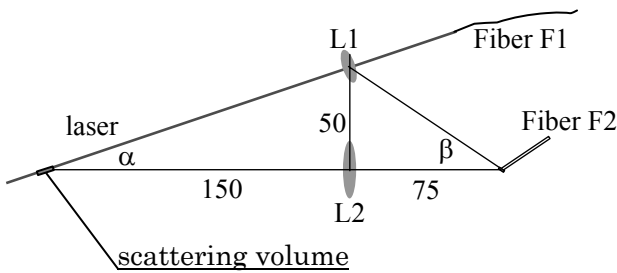


Fig. 2. Thomson scattering optics configuration.

An expanded view of the end of the optical fiber is shown in Fig. 3. The incident angle $\theta_1=90^\circ-\beta$ is chosen so that the light incident to the fiber is reflected as little as possible. If the laser beam and hence the scattered light is properly polarized (p-wave), the reflectance at the fiber surface is less than 1 % for $45^\circ<\theta_1<63^\circ$ as shown in Fig. 4. Unfortunately the fiber supposed to be used depolarizes the propagating laser light even if initially polarized. The unpolarized light reflects on the surface of the fiber by 5% on average for $45^\circ<\theta_1<63^\circ$ as shown in Fig. 4. We choose the central incident angle to be $\theta_1=56^\circ$ and hence $\beta=34^\circ$ and $\alpha=17^\circ$ for $m=0.5$. The end of the fiber is cut at 56° so that the central incident light propagates along the axis of the fiber after the refraction. A slit of 1mm in length and 0.5 mm in width set at the obliquely cut surface of the fiber defines the

scattering cylindrical volume of $L=3$ mm in length and $D=1$ mm in diameter located at the waist point of the laser beam shaped by L1 lens. The L1 lens has focal length $f=34$ mm and diameter $\phi 30$, which matches the $NA=0.22$ of the fiber F1 with the core diameter of 0.5 mm.

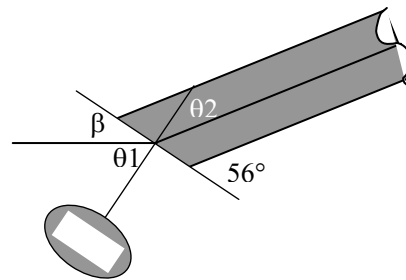


Fig. 3. Magnified view of the optical fiber for collecting TS-light.

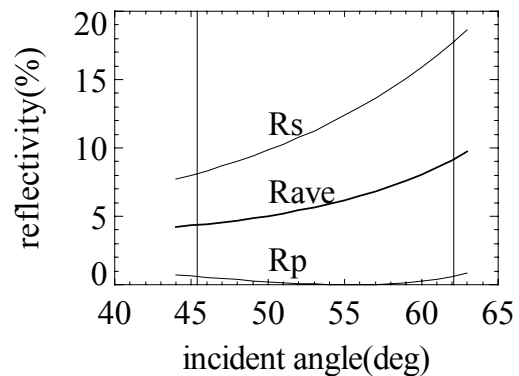


Fig. 4. Reflectivity at the end surface of the fiber as a function of incident angle.

The L2 lens has the focal length $f=52$ mm and 40 mm diameter with a $34\text{mm}\times 40$ mm square aperture which match the acceptance angle of the fiber F2. The aperture gives the solid angle of $\Delta\Omega=25$ msr. All optical components consisting the TS-probe is housed in a box of $100\times 100\times 50$ mm³ size. The scattering configuration is similar to a 1/20 model of the LHD-TS.

(2) Optical fiber: Two optical fibers are used: F1 is for delivering high power laser energy; and F2 is for transporting the scattered light to a polychromator.

Contrary to our intuition, it is reported that a step index type optical fiber made of pure silica can transmit a high power density [2]: A 400 μm core diameter fiber can transmit 2000 W CW light and a 1MW/mm² light pulse width <1ms. Considering available laser diode of 300W CW output, core diameter of 400 μm is large enough for F1 fiber. The f=52 mm lens (L1) with 20 \times 30mm² aperture focuses the scattered light onto the end surface of F2 fiber of 1mm in diameter cut at the Brewster angle. Both fibers set insides vacuum chamber is flexible enough enabling us to move the TS-probe head freely to a large extent. A simple metallic screen will shield the fiber against plasma radiation that would otherwise heats up the fibers. Unavoidable exposure to hard x-rays and neutrons, if present, will result in a gradual drop in the transmission of the fibers and fluorescent emission from the body of the fibers. The latter problem will not be serious for the present case in which a modulated laser beam is used. The former problem will be alleviated greatly by suitably selecting the fiber material and the wavelength of laser light (900-1100 nm) transmitted in the fiber. Raising the temperature of fibers, which may occur naturally or intentionally, will cure the defects introduced inside the fibers.

(3) **A Fiber feed-through** interfaces the fibers set in the inside and outside of a vacuum chamber. There is commercially available fiber feed-through that can be used for an ultra-high vacuum (UHV) environment of 10⁻¹⁰ mbar [3]. The durability against high power transmission is an issue not yet checked.

(4) **Laser diode:** A light source for a TS is required to be intense enough to yield sufficient signal and to have a wavelength width narrow enough to discern the Doppler broadening of the scattered spectrum due to thermal motion of plasma electrons. The allowable width ($\Delta\lambda$) depends on the minimum-measurable electron temperature T_{e_min} (eV) as follows: $\Delta\lambda/\lambda \ll T_{e_min}^{0.5}/500$. Examples: . for $T_{e_min}=10\text{eV}$, $\Delta\lambda/\lambda \ll 6/1000$; for $T_{e_min}=1\text{eV}$, $\Delta\lambda/\lambda \ll 2/1000$. These imply that it is not absolutely necessary to use lasers operating in a cavity, e.g., an Nd:YAG laser with $\Delta\lambda/\lambda \ll 10^{-6}$, as a TS-light source. Laser diodes, which are widely used for pumping the laser rod and for industrial

application such as welding and cutting, seem to be suitable for the present purpose. For example, LIMO GmbH produces a fiber coupled laser diode module that delivers 980 nm 350 W light from a 400 μm core fiber with NA=0.22 [4]. The specified line width (FWHM) $\Delta\lambda < 8$ nm will allow the Te measurement down to $T_{e_min} \sim 30\text{eV}$, which is rather high for edge plasma measurement. Recently it was reported [5] that a Bragg grating stabilizes a diode laser to yield power of 330 W from a fiber in $\Delta\lambda=0.5$ nm line width at $\lambda=967$ nm, which allowing a TS measurement down to a few eV. These above data are for a CW operation. As described later, the laser diode should be modulated at a high frequency. Whether there is degradation in high power delivering capability when used in modulation mode is an open question.

(5) **A polychromator** spectrum-analyze the scattered light transported by fibers. We will use a conventional three-filter polychromator. The principle of operation is based on the transmission and reflection characteristics of a combination of filters arranged to form a zigzag optical path. A key issue in the polychromator is to prevent the stray light with the wavelength at the laser from entering the light detector such as avalanche photo diode (APD). In the case of LHD-TS, each filter in the polychromator blocks the light at 1064 nm (Nd:YAG laser wavelength) with the blocking factor of 10⁵ (OD5). Even with this high blocking factor, some polychromators suffer from the stray light problem. Considering the absence of the beam dump in the present case, the filters with a much higher OD blocking will be necessary. A setting a notch filter with OD~4 at the laser wavelength at the exit of the fiber-lens may be a solution to this. In addition to the high blocking, the steepness of the edge of the filters is of importance related with the lowest detectable Te (T_{e_min}).

(6) **Lock-in amplifiers** are used to pickup weak scattered signals modulated at frequency f_m in the presence of an overwhelming background noise mainly arising from plasma light. In considering that the spectrum of plasma density fluctuation and the resultant plasma light fluctuation monotonically

decreases down to a sub-MHz region, the reference frequency f_m higher than 1MHz is favorable for reducing the noise contribution. There is a commercially available lock-in amplifier operating at frequency as high as 200 MHz: SR844 (Standard Research System) [6].

3. Signal to Noise Ratio

We suppose to measure a sheet like divertor leg plasma of 15 mm in depth that has Te less than 100 eV and ne ranging from 10^{18} m^{-3} to 10^{19} m^{-3} with a modulated laser diode of $P_{\text{LASER}}=300\text{W}$ and $\lambda_{\text{LASER}}=980 \text{ nm}$.

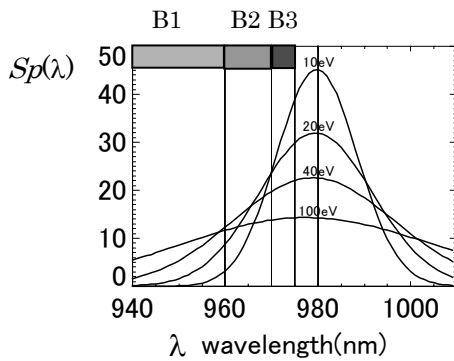


Fig. 5. TS spectra for various Te . Three color bands are indicated.

The backward TS spectrum is shown in Fig. 5 for various Te , which are discriminated by three color channels with pass bands B1=[940, 960], B2=[960, 970] and B3=[970, 975] in nm unit. The light power fed to a polychromator is the sum of the scattered light P_{sct} plus the plasma radiation P_{rad} , which are given respectively as

$$P_{\text{sct}} = P_{\text{LASER}} ne L (d^2\sigma/d\Omega d\lambda) \Delta\Omega \Delta\lambda$$

$$\approx 1.2 (P_{\text{LASER}}/300\text{W}) (ne/10^{19} \text{ m}^{-3}) (L/3\text{mm})$$

$$*(\Delta\Omega/25\text{msr}) Sp(\lambda) d\lambda/\lambda_{\text{LASER}} \text{ pW} \quad (1)$$

and

$$P_{\text{rad}} = j_v \Delta v \Delta V \Delta \Omega$$

$$\approx 110 (Z_{\text{eff}}/3) (ne/10^{19} \text{ m}^{-3})^2 (Te/100\text{eV})^{-1/2} * (G/10)$$

$$(\Delta\Omega/25\text{msr}) (V_{\text{obs}}/10\text{mm}^3) * (\Delta\lambda/\text{nm}) (1\mu\text{m}/\lambda)^2 \quad (2)$$

Here $Sp(\lambda)$ is the TS spectrum shown in Fig. 5, $\lambda_{\text{LASER}}=980 \text{ nm}$ is the laser wavelength, j_v is the Bremsstrahlung emissivity, Z_{eff} is the effective ion charge, G is the Gaunt factor enhanced ~ 5 times to take account of enhanced radiation due to recombination and line radiation, $V_{\text{obs}} \sim \pi D^2/4 * 15 \sim 10\text{mm}^3$ is the effective plasma volume that the collection optics see. The light power that falls in i -th filter's pass band is incident to the i -th APD, inducing a current

$$j_i = \int d\lambda (P_{\text{sct}} + P_{\text{rad}}) F_i(\lambda) / h\nu$$

$$= \int d\lambda (P_{\text{sct}} + P_{\text{rad}}) F_i(\lambda) / \lambda / hc \quad (3)$$

$$\equiv j_{\text{si}} + j_{\text{bi}}$$

Here $F_i(\lambda)$ is the filter transmittance η_{FIL} times quantum efficiency η_Q of the i -th channel: $F_i(\lambda) = \eta_{\text{FIL}}(\lambda) \eta_Q(\lambda)$. We assume an idealized filter with $\eta_{\text{FIL}} = 0.9$ in the i -th pass band and $\eta_{\text{FIL}} = 0$ otherwise. The responsivity (A/W) and its associated quantum efficiency η_Q (%) of an APD are shown in Fig. 7 as function of wavelength, from which we reasonably set $\eta_Q = 0.75$ for the three pass bands (940 nm $< \lambda < 975$ nm).

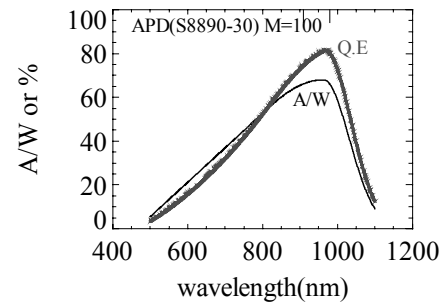


Fig. 6. Responsivity and quantum efficiency of an APD (Hamamatsu S8890).

For later use, we define x_i by

$$x_i \equiv j_{\text{si}} / ne \quad (4)$$

Figure 7 (a) and (b) show j_{bi} and j_{si} for plasma with $ne = 10^{19} \text{ m}^{-3}$ as a function of Te . We note that the scattering signals $\{j_{\text{si}}; i=1,2,3\}$ are deeply buried in the plasma Bremsstrahlung signals $\{j_{\text{bi}}; i=1,2,3\}$. The outputs of the APDs, which is proportional to $j_i = j_{\text{si}} + j_{\text{bi}}$ are fed to three lock-in amplifiers. A lock-in

amplifier is a kind of a Fourier analyzer if the reference input is fed by a precise sinusoidal signal, which is also used to modulate the laser diode. The frequency spectrum of the output of an APD is composed of two terms: one is a very narrow TS-signal centered at the modulation frequency f_m ; other is broad band noise mainly generated by shot noise. The current in the APD $j_i = j_{si} + j_{bi} + j_d$ generates the shot noise whose power spectrum is given by

$$\langle i_n^2 \rangle = 2e(j_{si} + j_{bi} + j_d)M^2Fn(M)\Delta f. \quad (5)$$

where $M \sim 100$ is the multiplication factor of the APDs and $j_d \sim 1$ nA is the dark current in the APD, $Fn(M)$ is an excess noise factor and Δf is the bandwidth.

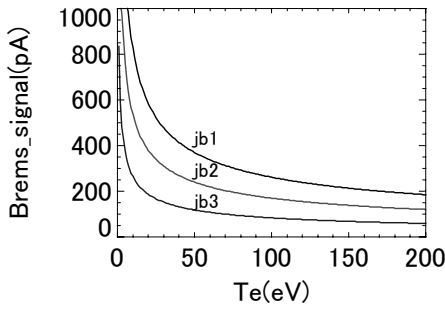


Fig.7 (a) APD currents induced by Bremsstrahlung.
 $ne=10^{-19}m^{-3}$.

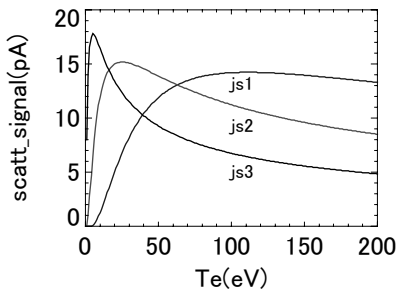


Fig.7 (b) APD currents induced by Thomson scattered light. $ne=10^{-19}m^{-3}$.

The appearance of $Fn(M)$ implies an enhanced noise in the avalanche process in APD [7,8,9]. $Fn(M)$ is dependent on the ratio of hole ionization to electron

ionization. By suitable design and selection of processing material, $Fn(M)$ can be less than 4 for $M=100$ [9]. In this paper we assume $Fn(M)=10$. The RC-type integration time τ of a lock-in amplifier gives the spectrum width Δf given by the relation $\Delta f=1/4\tau$. Then, the output of the lock-in amplifier is expressed as

$$y_i = j_{si} \pm [e(j_{si} + j_{bi} + j_d)/2\tau]^{1/2} \equiv j_{si} \pm \delta_i. \quad (5)$$

Hence, however deeply the TS-light is buried in the plasma radiation, it is possible to pickup the TS-signal by taking a long enough integration time. With these data $\{y_i; i=1,2,3\}$ we can estimate the errors on the deduced Te and ne by following the standard method. The two ratios $j_{s1}/j_{s3} \equiv g1(Te)$ and $j_{s2}/j_{s3} \equiv g2(Te)$ are functions of Te alone as shown in Fig. 8. Conversely, the observed ratios $y1/y3$ and $y2/y3$ give two Te : $Te1 = g^{-1}(y1/y3)$ and $Te2 = g^{-1}(y2/y3)$. Here g^{-1} is the inverse function of g .

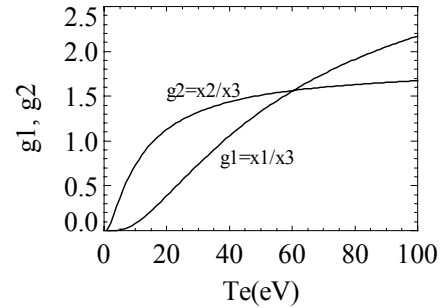


Fig. 8. Two ratios among the TS-signals from three-color channels.

The errors on $Te1$ and $Te2$ are calculated as

$$(\delta Te1)^2 = (\partial g1^{-1}(x)/\partial x)^2 (\delta y1^2/y3^2 + y1^2 \delta y3^2/y3^4) \quad (6)$$

$$(\delta Te2)^2 = (\partial g2^{-1}(x)/\partial x)^2 (\delta y2^2/y3^2 + y2^2 \delta y3^2/y3^4) \quad (7)$$

$$(\delta y_i)^2 = e(j_{si} + j_{bi} + j_d)/2\tau \quad (6)$$

With the variance $(\delta Te)^2$ defined by

$$1/(\delta Te)^2 = 1/(\delta Te1)^2 + 1/(\delta Te2)^2 \quad (8)$$

the most probable Te is given by

$$Te = (Te1/(\delta Te1)^2 + Te2/(\delta Te2)^2) / (\delta Te)^2 \quad (9)$$

The errors on ne is obtained, for example, from

$$ne = j_{s3} / x_3 \quad (10)$$

$$(\delta ne / ne)^2 = (\delta j_{s3} / j_{s3})^2 + (\partial x_3(Te) / \partial Te)^2 (\delta Te)^2 \quad (11)$$

In what follows, we shows relative errors in Te and ne , $\sqrt{(\delta Te)^2 / Te}$ and $\sqrt{(\delta ne)^2 / ne}$, as a function Te for several combinations of parameters that gives the relative errors less than 20%. First we show the relative errors for $P_{LASER}=300W$, $ne=10^{19}m^{-3}$ and $\tau=0.1s$ in Fig. 9. Errors in both Te and ne are less than 10% for $6eV < Te < 90eV$. This implies that a plasma with $ne \geq 10^{19}m^{-3}$ can be measured with time resolution around 0.1s.

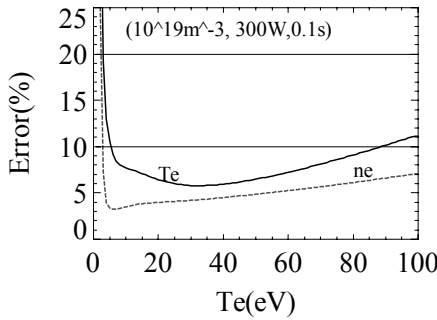


Fig. 9. $\sqrt{(\delta Te)^2 / Te}$ and $\sqrt{(\delta ne)^2 / ne}$ for $P_{LASER}=300W$, $ne=10^{19}m^{-3}$ and $\tau=0.1s$.

For a ten times more dense plasma, $ne=10^{20}m^{-3}$, an integration time of 0.05 s is necessary for the same $P_{LASER}=300W$ as shown in Fig. 10.

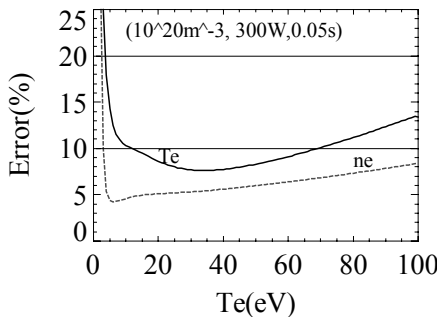


Fig.10. $\sqrt{(\delta Te)^2 / Te}$ and $\sqrt{(\delta ne)^2 / ne}$ for $P_{LASER}=300W$, $ne=10^{20}m^{-3}$ and $\tau=0.05s$.

Even a smaller laser power of $P_{LASER}=100W$ yields a reasonable data quality with a longer integration time of 0.5 s as shown in Fig. 11.

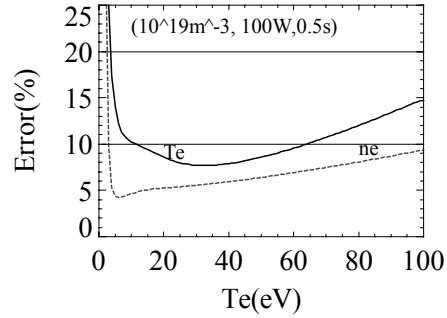


Fig.11. $\sqrt{(\delta Te)^2 / Te}$ and $\sqrt{(\delta ne)^2 / ne}$ for $P_{LASER}=100W$, $ne=10^{19}m^{-3}$ and $\tau=0.5s$.

Even lower density plasma of $ne=10^{18}m^{-3}$ can be measured with $P_{LASER}=300W$ by integrating much longer time of 1 s as shown in Fig.12.

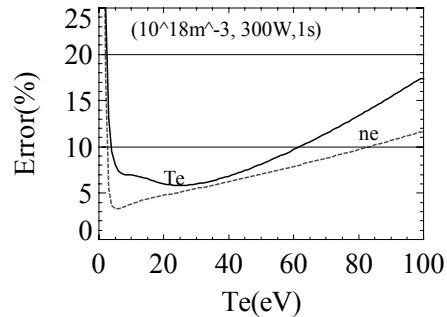


Fig.12. $\sqrt{(\delta Te)^2 / Te}$ and $\sqrt{(\delta ne)^2 / ne}$ for $ne=10^{18}m^{-3}$, $P_{LASER}=300W$ and $\tau=1s$.

4. Discussions

We showed the feasibility of a TS-probe based on optical fibers and the recently developed high power laser-diode with narrow line width. It was shown that the currently available laser diode of 300W can yield accurate Te and ne data for plasma of $ne \sim 10^{19}m^{-3}$ with integration time of 0.1s. If there were no enhancement in APD noise, the noise power spectrum in Eq. (5) is proportional to M^2 . In this case, the errors in Te and ne are much reduced and

an integration time of 0.01 s is long enough to yield accurate data as shown in Fig.13.

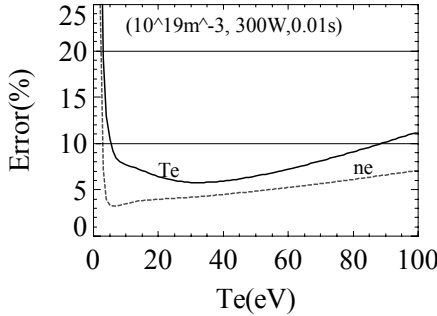


Fig.13. $\sqrt{(\delta Te)^2}/Te$ and $\sqrt{(\delta ne)^2}/ne$ for $P_{LASER} = 300W$, $ne = 10^{19} m^{-3}$ and $\tau = 0.01s$ when no enhanced noise is added to APDs.

In this view, developing photo detectors with smaller noise are worthwhile [9]. With the presently available APDs, time integration longer than 0.1 s is necessary for measuring plasma with $10^{19} m^{-3} \geq ne$. Hence, the proposed TS-probe is suitable only for long pulse discharge experiments. For measuring a fast phenomenon a shorter integration time less than 0.1s is desirable. A way to improve this is to raise the TS-light power. The key element of the TS-probe is intense light transmission in a fiber. A $\phi 1.2$ fiber, which is still flexible, can transmit light of 2kW CW and 1MW pulse with duration less than 1ms. If 1MW laser of 0.1 ms pulse width is available, it will give enough accuracy with $\tau = 0.01$ ms as shown in Fig.14.

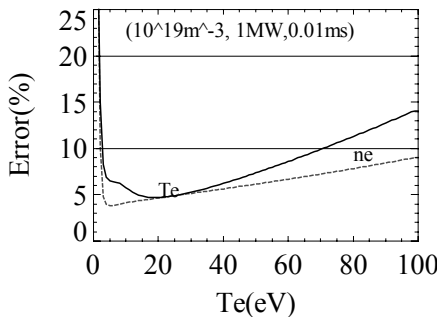


Fig.14. $\sqrt{(\delta Te)^2}/Te$ and $\sqrt{(\delta ne)^2}/ne$ for $P_{LASER} = 1MW$, $ne = 10^{19} m^{-3}$ and $\tau = 0.01ms$.

Up to this point, we have assumed that there is no plasma light fluctuation around the frequency of the laser diode modulation $f_m \sim 1MHz$. This assumption may be supported by the fact that there is no success report on detecting turbulent density fluctuation by Bremsstrahlung measurement. A key point in the present TS-probe is the smallness of $V_{obs} \sim 10mm^3$, which helps to reduce the plasma radiation power entering to the light collection optics. This is accomplished by matching the slit size on the light collecting fiber to the size of the image of the laser beam whose size is reduced down to $\phi 1mm$. The beam size largely depends on the fiber diameter and the N.A. The smaller diameter and smaller NA are favorable for reducing the beam size. If it is possible to mount a laser diode on the TS-probe head, the beam size at the focal point can be reduced much less than $\phi 0.1$, thus lowering V_{obs} and P_{rad} several orders of magnitude. This approach of design will be given elsewhere.

REFERENCES

- [1] K. Narihara, et al., Fusion Engineering and Design **34-35**, 67 (1997).
- [2]Diaguide, Mitsubishi-cable Catalog 2000.07 (in Japanese).
- [3] www.lewvac.co.uk
- [4] www. LIMO.de
- [5] Laser Focus World Japan 2008-8, p52.
- [6] www. Thinkers.com/products/SR844.htm
- [7] A. van der Ziel, *Noise*, Prentice-Hall, Inc, 1954.
- [8] R.J. McIntyre, IEEE Trans. on Electron Devices, **ED-13**, 164 (1966).
- [9] ‘The Avalanche Photodiode Catalog’, Advanced Photonix, Inc.